Acta Cryst. (1987). B43, 567-574

The Incommensurately Modulated Structure of the Triclinic Form of *N*,*N*-Dimethylmorpholinium Di-7,7,8,8-tetracyano-*p*-quinodimethanide; DMM(TCNQ)$_2$(II) at 99 K

BY W. STEURER

Institut für Kristallographie und Mineralogie der Universität, Theresienstrasse 41, *D*-8000 *München* 2, *Federal Republic of Germany*

AND R. J. J. VISSER, S. VAN SMAALEN AND J. L. DE BOER

Materials Science Centre, Department of Inorganic Chemistry, Nijenborgh 16, 9747 *AG Groningen, The Netherlands*

(*Received* 9 *February* 1987; *accepted* 11 *May* 1987)

Abstract

The triclinic form of DMM(TCNQ)$_2$, space group $P\bar{1}$ at room temperature, transforms below 207 K to an incommensurately modulated phase. Its crystal structure has been determined at 99 K: $C_6H_{14}NO^+.2C_{12}H_4N_4^{1/2-}$, $M_r = 524{\cdot}6$, superspace group $P^{P\bar{1}}_{1}$ [$-0{\cdot}046\,(4)$, $0{\cdot}465\,(5)$, $0{\cdot}385\,(3)$], $a = 16{\cdot}452\,(3)$, $b = 12{\cdot}838\,(3)$, $c = 6{\cdot}592\,(2)$ Å, $\alpha = 103{\cdot}18\,(2)$, $\beta = 98{\cdot}79\,(2)$, $\gamma = 103{\cdot}25\,(2)°$, $V = 1288$ Å^3, $Z = 2$, $D_x = 1{\cdot}352$ Mg m^{-3}, Mo $K\bar{\alpha}$, $\lambda = 0{\cdot}71069$ Å, $\mu = 0{\cdot}095$ mm^{-1}, $F(000) = 546$, $wR(F) = 0{\cdot}037$ for 12 291 independent reflections [$wR(F) = 0{\cdot}122$ for the 4790 satellite reflections of first order]. At room temperature, the DMM molecules, in chair conformations, are randomly disordered. At 99 K, the DMM groups are almost completely ordered in an incommensurate way and are accommodated in the channels formed by the TCNQ stacks by a small displacive modulation of the latter. Some physical implications of the structural changes are discussed.

Introduction

TCNQ forms charge-transfer complexes with a large variety of both organic and inorganic donors (see, for example, Melby, Harder, Hertler, Mahler, Benson & Mochel, 1982). Many of them have been investigated structurally to obtain more insight into the relations between crystal structure and physical properties, with the ultimate aim of designing compounds with *a priori* desired properties.

Pure structural influence on physical properties can best be studied if one compound exists in several modifications as is the case for DMM(TCNQ)$_2$, which crystallizes from acetonitrile in both a monoclinic (I) and a triclinic (II) form. The room-temperature structure of (I) has been solved by Kamminga & van Bodegom (1981) and of (II) by Visser, de Boer & Vos (1987). Now, for example, the difference in the electrical conductivity of the room-temperature phases (I) and (II) by nearly two orders of magnitude (Visser, van Heemstra & de Boer, 1982) can be explained.

It is an interesting fact that forms (I) and (II) both undergo phase transitions on cooling. Recently, the structure of (I) at 95 K has been published (Middeldorp, Visser & de Boer, 1985). For (II), a transition at 1·7 K to an antiferromagnetic phase was found by Korving, Hijmans, Brom, Oostra, Sawatzky & Kommandeur (1983), but no anomalies in the electrical conductivity and the spin susceptibility between room temperature and say 100 K were detected. Nevertheless, form (II) develops an incommensurate phase on cooling below 207 K, as was discovered by X-ray diffraction. The determination of this modulated structure was undertaken to obtain information about the expected ordering of the DMM groups, accompanied by a possible modulation of the TCNQ stacks, which effects might be connected with the ultimate transition to the antiferromagnetic phase.

Experimental

The incommensurate character of (II) at low temperature was first observed on oscillation photographs and subsequently confirmed on a CAD-4F diffractometer, on a single crystal carefully selected from the abundantly present twin crystals. From inspection of very strongly exposed films, the existence of at least a few higher-order satellites is beyond doubt, but on the diffractometer only first-order satellites could be collected. The intensities of the 31 strongest satellites were measured as a function of temperature on the CAD-4F diffractometer. Their average intensity as a function of temperature is plotted in Fig. 1, showing that the transition has its onset T_i around 207 K. In the temperature range studied, no

0108-7681/87/060567-08$01.50

temperature dependence, within the standard deviation, of the modulation vector **q** could be detected. At 99 K, from 25 optimized satellite reflections, **q** was determined as $\mathbf{q} = -0{\cdot}046\,(4)\mathbf{a}^* + 0{\cdot}465\,(5)\mathbf{b}^* + 0{\cdot}385\,(3)\mathbf{c}^*$. At the same temperature, all intensity data were collected with Mo $K\bar{\alpha}$ radiation, on the CAD-4F diffractometer provided with graphite monochromator, beam flattener (Helmholdt & Vos, 1977) and a modified CAD-4 program (de Boer & Duisenberg, 1984); up to $\theta = 30°$, 7501 main reflections of which 907 had $I = 0$; up to $\theta = 20°$, 4790 first-order satellites, of which 1140 had $I = 0$. Corrections for intensity control were within ±2·1%. All data were corrected for Lorentz and polarization effects but not for absorption. From these data, the low-temperature structure at 99 K was determined in an average form (Visser *et al.*, 1987) disregarding the satellite reflections and without bond-length constraints for the split DMM group.

Refinement and results

The average structure of (II) at 99 K was refined in $P\bar{1}$ by splitting the DMM molecule in its two possible chair conformations (DMM-1 and DMM-2, in such a way as to leave the O and N positions relatively untouched) and applying soft constraints to this splitting, in the sense that, for both chairs, chemically equivalent N–C, O–C and C–C bonds were kept equal within 0·01 Å, to avoid high correlations. The H atoms were assigned variable isotropic temperature factors and were constrained at 1·08 Å from the respective C atoms.

The calculations were performed with the program *SHELX* (Sheldrick, 1976). Anomalous-dispersion corrections and atomic scattering factors were taken from *International Tables for X-ray Crystallography* (1974). A weighting scheme $w(F) = 1/\sigma^2(F)$ was applied. This refinement resulted in $R = 0{\cdot}102$, $wR = 0{\cdot}041$ for 6594 contributing reflections ($I > 0$) and 474 variables. Keeping in mind the quite anisotropic thermal expansion of TCNQ stacks (van Smaalen, de Boer, Haas & Kommandeur, 1985), one finds that a comparison of this average low-temperature structure with the room-temperature structure does not show essential differences between the TCNQ parts of the structures. The split for the DMM moieties, however, already present in the room-temperature model, becomes even larger at 99 K.

When interpreting the smearing phenomena in the average low-temperature structure as resulting from ordering effects below T_i, it is clear that the DMM group has a major contribution. Its ordering could roughly be described by a displacive modulation wave with high amplitude (about 0·5 Å) transforming one chair conformation to the other, or equivalently by two density modulation waves of the DMM moieties with a phase difference of $\Delta T = 0{\cdot}5$ (Fig. 2). In order to check the validity of this model and to get an idea about the modulation (if any) of the TCNQ molecules, it was necessary to employ (3+1)-dimensional Patterson functions [(3+1)-PF] as discussed by Steurer (1987). According to the superspace theory of de Wolff (1974), one-dimensionally modulated structures can be described in a fictitious four-dimensional lattice. The unit cell in this superspace contains the atoms as continuous strings ('string atoms') with the shape of the modulation function in the extra dimension $\mathbf{e}_4$. The (3+1)-PF represents the vector function between these 'string atoms' yielding information about the phase difference and the amplitude sums of the atoms involved. It is centrosymmetric and a continuous function in the extra dimension. The projection of the (3+1)-PF along $\mathbf{e}_4$ gives the Patterson map of the average structure.

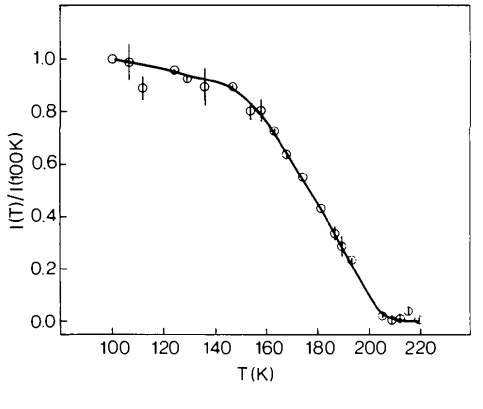

Fig. 1. Temperature dependence of the satellite intensities of DMM(TCNQ)$_2$.

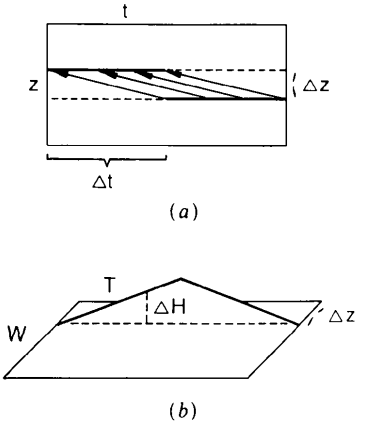

Fig. 2. (*a*) Schematic drawing of a (1+1)-dimensional unit cell containing two 'string atoms' with the shape of a box function (full line: occupancy 1, broken line: occupancy 0) and a phase difference of $\Delta t = 0{\cdot}5$. A completely equivalent description would be a rectangular shift modulation wave. The number of equivalent vectors between the string atoms depends on the component Δt and is maximal for $\Delta t = 0{\cdot}5$ (some vectors plotted) and minimal for $\Delta t = 0$. The shape of this vector function is triangular and illustrated in the (3+1)-PF shown in (*b*).

Therefore, if the Patterson map of the average structure shows well resolved peaks for a particular interaction it might be promising to investigate the (3+1)-PF around this region.

To find the most expressive regions in our case, all possible Patterson vectors of the average structure were calculated with the aid of a small computer program. But even within the selected regions one is left with problems caused by substantial overlap of the peaks. In Fig. 3 some sections of the (3+1)-PF

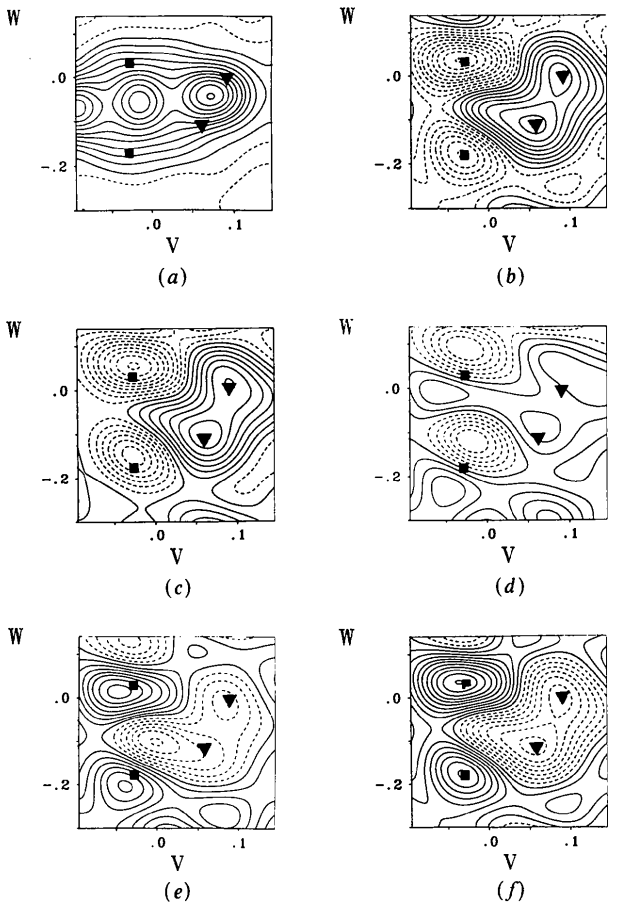

Fig. 3. (*a*) Section through a Patterson synthesis ($U = 0{\cdot}96$) calculated from the main reflections. The map is dominated by the maxima corresponding to a high number of superposed vectors between neighbouring atoms of DMM and TCNQ molecules. The same sections, now through the (3+1)-PF calculated from the satellite reflections alone, are plotted for the phase terms (*b*) $T = 0$, (*c*) $T = 0{\cdot}125$, (*d*) $T = 0{\cdot}25$, (*e*) $T = 0{\cdot}375$ and (*f*) $T = 0{\cdot}5$. Now, in contrast to (*a*), modulated atoms contribute to the pattern only and the principal information that the DMM as well as the TCNQ molecules are modulated is obtained easily. The region around the squares is characterized by the vectors between the split atoms of the DMM moieties [upper square: C(341)-C(342),...; lower square: C(341)-C(352),...]. The (3+1)-PF peaks corresponding to the intramolecular vectors of the TCNQ molecules like C(8)-C(9), C(24)-(C25),... are superposed in the surroundings of the triangles. A maximum at $T = \Delta t = 0$ corresponds to a phase difference of 0 and a minimum to a phase difference of 0·5 of the modulation waves of the atoms involved (*cf.* Fig. 2).

Table 1. *R values for the successive stages of the structure refinement*

(*a*) Average structure
$R = 0{\cdot}102$, $wR = 0{\cdot}041$ for 6594 reflections ($I > 0$) and 474 variables
(*b*) Modulated structure: DMM molecule unsplit and displacively modulated
$R = 0{\cdot}152$, $wR = 0{\cdot}109$ for 3613 main and satellite reflections
$R = 0{\cdot}116$, $wR = 0{\cdot}096$ for 2072 main reflections [$I > 10\sigma(I)$]
$R = 0{\cdot}462$, $wR = 0{\cdot}501$ for 1541 satellite reflections [$I > 2\sigma(I)$]
(*c*) In addition, all atoms of the TCNQ molecules displacively modulated
$R = 0{\cdot}138$, $wR = 0{\cdot}099$ for 3613 main and satellite reflections
$R = 0{\cdot}087$, $wR = 0{\cdot}091$ for 2072 main reflections [$I > 10\sigma(I)$]
$R = 0{\cdot}378$, $wR = 0{\cdot}377$ for 1541 satellite reflections [$I > 2\sigma(I)$]
(*d*) Final model: shift and density modulation for the split DMM moieties and displacive modulation for the atoms of the TCNQ molecules
$R = 0{\cdot}161$, $wR = 0{\cdot}037$ for 12 291 main and satellite reflections ($I \geq 0$) and 779 variables
$R = 0{\cdot}116$, $wR = 0{\cdot}035$ for 7501 main reflections ($I \geq 0$)
$R = 0{\cdot}369$, $wR = 0{\cdot}122$ for 4790 satellite reflections ($I \geq 0$)
(*e*) The values $eR = \sum \sigma(F)/\sum F(\text{obs.})$ as an estimation for the best reachable R values are:
$eR = 0{\cdot}044$ for the main reflections with $I > 2\sigma(I)$
$eR = 0{\cdot}113$ for the satellites with $I > 2\sigma(I)$

are shown giving information about interactions between atoms of DMM-1 and DMM-2 as well as between atoms of the TCNQ molecules. If our model is correct then the (3+1)-PF (calculated from the satellite intensities alone) should give a maximum at $T = 0{\cdot}5$ for the DM-1-DMM-2 interaction. Indeed, the shape of the (3+1)-PF is in accordance with the expected one (see Fig. 2). The peaks marked by triangles in Fig. 3 indicate a modulation of the TCNQ molecules. Since the maximum of the (3+1)-PF for this interaction is found at $T = 0$ there are no phase differences between the modulation functions of the involved atoms of the TCNQ molecules and a phase difference of $T = \Delta t = 0{\cdot}5$ relative to the DMM modulation. Therefore, one can expect that, once having found the DMM modulation, small arbitrary starting amplitudes and equal phases for the modulation of the TCNQ groups will smoothly converge to real values.

A survey of the successive stages of the structure refinement and the corresponding R factors is given in Table 1. It should be noted that the (3+1)-dimensional Fourier function [(3+1)-FF] (Steurer, 1987) was an indispensable instrument in all steps of the structure determination to find the correct, physically significant, modulation parameters describing the combined displacive and occupational modulation.

The refinements of the modulated structure have been carried out, using the main reflections and the first-order satellite reflections, with the program described by Steurer & Adlhart (1983). The structure-factor formula used is given in Table 2 (the derivation of this formula is demonstrated in the Appendix*).

* This Appendix and lists of structure factors have been deposited with the British Library Document Supply Centre as Supplementary Publication No. SUP 44254 (32 pp.). Copies may be obtained through The Executive Secretary, International Union of Crystallography, 5 Abbey Square, Chester CH1 2HU, England.

Table 2. *Structure-factor formula for general harmonic shift and density modulation used in the refinements*

A derivation of this equation is given in the Appendix (deposited). $\mathbf{Q} = h\mathbf{a}^* + k\mathbf{b}^* + l\mathbf{c}^* + m\mathbf{q}$, $\mathbf{q} = \alpha\mathbf{a}^* + \beta\mathbf{b}^* + \gamma\mathbf{c}^*$, $f_k(\mathbf{Q})$ is the scattering factor for the atom k, $T_k(\mathbf{Q})$ the temperature factor, $\mathbf{r}_k$ the positional vector of the atom k, $J_m(w_k)$ a Bessel function of mth order.

$$w_k = -(QAS)_k/\cos(\chi_k),\ \chi_k = \arctan[-(QAC)_k/-(QAS)_k],$$

$$(QAC)_k = \mathbf{Q}[A_k^x \cos(2\pi\varphi_k^x) + A_k^y \cos(2\pi\varphi_k^y) + A_k^z \cos(2\pi\varphi_k^z)]$$

and

$$(QAS)_k = \mathbf{Q}[A_k^x \sin(2\pi\varphi_k^x) + A_k^y \sin(2\pi\varphi_k^y) + A_k^z \sin(2\pi\varphi_k^z)].$$

The components of the displacive modulation are

$$A_k^x \sin[2\pi(\mathbf{q}\,.\,\mathbf{r}_{kl} + \varphi_k^x)],$$

$$A_k^y \sin[2\pi(\mathbf{q}\,.\,\mathbf{r}_{kl} + \varphi_k^y)],$$

$$A_k^z \sin[2\pi(\mathbf{q}\,.\,\mathbf{r}_{kl} + \varphi_k^z)].$$

The density modulation is defined as

$$p'_{kl}(\mathbf{q}\,.\,\mathbf{r}_{kl}) = 0{\cdot}5\{1 + A_k^p \sin[2\pi(\mathbf{q}\,.\,\mathbf{r}_{kl} + \varphi_k^p)]\}.$$

l is the index of the cell.

$$F_m(\mathbf{Q}) = \delta(\mathbf{Q} - \mathbf{H} - m\mathbf{q}) \sum_k \tfrac{1}{2} f_k(\mathbf{Q}) T_k(\mathbf{Q})$$
$$\times \exp(2\pi i \mathbf{H}\,.\,\mathbf{r}_k - \tfrac{1}{2} im\pi)\{J_m(w_k)\exp(im\chi_k)$$
$$-\tfrac{1}{2}A_k^p J_{m+1}(w_k)\exp[i(m+1)\chi_k + 2\pi i\varphi_k^p]$$
$$+ J_{m-1}(w_k)\exp[i(m-1)\chi_k - 2\pi_i\varphi_k^p)]\}$$

A conventional weighting scheme $w(F) = 1/\sigma^2(F)$ was applied. The same soft bond-length constraints have been included as for the refinement of the average structure, but, as an additional condition, the constrained distances were only allowed to vary within ±0·01 Å during the whole modulation period. The final atomic parameters are listed in Table 3. The high isotropic temperature factor of H(374) may indicate that the CH_2 groups slightly rotate during a modulation period whereas the chosen constraints allow parallel shifts of the C and H atoms only. The mispositioning of an atom will be compensated by a high thermal parameter in such a case. The F(obs.)/F(calc.) plots (Fig. 4) show quite a similar distribution for satellite and main reflections of comparable magnitude. Therefore, the higher R value for the satellite reflections may be due to the worse counting statistics of the weak satellite intensities rather than, compared with the quality of the basic structure, a worse fit of the modulation model. An illustration of the result that the modulation of the DMM group has to be described by a shift and a density wave at the same time is given in Fig. 5. The dependency of the intraatomic distances in the TCNQ molecules on the modulation phase is shown in Fig. 6. The bond lengths of TCNQ B exhibit larger variations than those of TCNQ A. This may be a consequence of the deeper penetration of TCNQ B into the electropositive regions of the DMM cations compared with TCNQ A.

Discussion

The variation in conformation and position of the DMM molecule as a function of the wave phase is demonstrated in Fig. 7 and in Fig. 8 an idea is given of how the crystal structure is disturbed by the ordering of the DMM molecules and the corresponding distortion of the TCNQ stacks.

The ordering of the DMM groups is not complete in the harmonic description used. From the refinements of the average structure the occupancy factors for DMM-1 and DMM-2 were found to be 0·55 and 0·45, respectively. The amplitudes of the density modulation waves [0·86 (2) and 1·05 (2)] indicate that at 99 K about 95% (0·55 times 0·86 plus 0·45 times 1·05 gives the density modulated fraction of 0·95) of the DMM groups are periodically alternating between the possible chair conformations. Therefore, 5% are still left distributed statistically in the DMM-1 conformation. How can this be explained?

It is clear that the ordering of the DMM molecules destroys the centre of symmetry present at room temperature between the DMM neighbours fluctuating dynamically from chair 1 to chair 2. For neighbouring DMM molecules (see Fig. 8) around the inversion centre i at $\frac{1}{2}\frac{1}{2}\frac{1}{2}$, there are now four possible combinations DMM-1–DMM-1^i, DMM-1–DMM-2^i, DMM-2–DMM-1^i and DMM-2–DMM-2^i, of which the latter is unfavourable for steric reasons. Fig. 9 shows how the unfavourable combination can largely (the abovementioned 95%) be avoided with a simple regular alternation of the DMM conformations using the phases of the modulation waves as resulting from the structure refinements. If a fluctuation of the phases of the modulation waves is allowed, the unfavourable combination can be avoided completely. A fully ordered arrangement of the favourable DMM conformations can be obtained with an asymmetric (0·55:0·45) modulation function as demonstrated in Fig. 9. The present experimental data do not allow one to decide between these possibilities considering local order (a long-range-ordered asymmetric rectangular wave can be excluded because no strong higher-order satellites can be observed on the diffraction patterns) but strongly support models with statistical phase fluctuations. Periodic phase fluctuations (phasons) can be excluded since overexposed Weissenberg photographs (at 125 K) do not show any diffuse scattering around the satellite reflections as would be expected in that case (Adlhart, 1982). Only a few rather sharp streaks parallel to $\mathbf{b}^*$ are observable around the strong main reflections $0\bar{2}2$, $0\bar{1}2$, 002 and 010 indicating some kind of static disorder (the same streaks, accompanied by diffuse regions, can be observed in the room-temperature diffraction pattern).

As to the distortion of the TCNQ stacks, a characteristic feature is the relatively large deformation of

Table 3. *Fractional atomic coordinates* ($\times 10^4$), *occupancy factor p, anisotropic temperature factors* ($Å^2 \times 10^3$), *amplitudes* (*in fractions of a, b, c,* $\times 10^3$) *and phases* (*in fractions of one period,* $\times 10^2$) *of the shift waves, amplitudes* ($\times 10^2$) *and phases* ($\times 10^2$) *of the density waves; e.s.d.'s in parentheses*

The anisotropic temperature factor

$$T = \exp[-2\pi^2(U_{11}h^2a^{*2} + U_{22}k^2b^{*2} + U_{33}l^2c^{*2} + 2U_{12}hka^*b^* + 2U_{13}hla^*c^* + 2U_{23}klb^*c^*].$$

	x	y	z	p	U_{11}	U_{22}	U_{33}	U_{12}	U_{13}	U_{23}	A^x	A^y	A^z	φ^x	φ^y	φ^z	A^p	φ^p
N(331)	3511 (1)	3369 (1)	−3808 (1)	0·55	11 (1)	18 (1)	21 (1)	2 (1)	10 (1)	1 (1)	−5 (1)	10 (1)	27 (1)	39 (1)	−17 (1)	89 (1)	86 (2)	19 (1)
N(332)	3290 (1)	3317 (1)	−3547 (1)	0·45	29 (1)	40 (1)	17 (1)	26 (1)	18 (1)	21 (1)	2 (1)	2 (1)	−14 (1)	−12 (1)	−10 (1)	14 (1)	105 (2)	67 (1)
C(341)	3501 (1)	4441 (1)	−2266 (1)	0·55	15 (3)	19 (3)	18 (4)	8 (3)	12 (3)	12 (3)	6 (1)	5 (1)	41 (1)	73 (2)	70 (2)	75 (1)	86	5 (1)
C(342)	3189 (1)	4185 (1)	−1691 (1)	0·45	13 (4)	18 (4)	48 (6)	6 (3)	11 (4)	3 (4)	9 (1)	7 (1)	14 (1)	6 (1)	1 (1)	47 (1)	105	53 (1)
C(351)	3489 (1)	4337 (1)	−28 (1)	0·55	11 (3)	15 (3)	6 (4)	1 (3)	0 (3)	−1 (3)	10 (1)	9 (1)	44 (1)	59 (1)	56 (1)	66 (1)	86	−3 (1)
C(352)	3972 (1)	4874 (1)	−15 (1)	0·45	27 (5)	32 (5)	39 (6)	14 (4)	−2 (5)	4 (5)	4 (1)	−5 (1)	−9 (1)	−3 (2)	61 (1)	−50 (2)	105	47 (1)
O(361)	4185 (1)	3982 (1)	839 (1)	0·55	24 (3)	18 (3)	20 (3)	0 (2)	11 (2)	6 (2)	13 (1)	−11 (1)	35 (1)	63 (1)	8 (1)	59 (1)	86	−5 (1)
O(362)	4415 (1)	4174 (1)	766 (1)	0·45	25 (3)	14 (3)	15 (3)	10 (2)	13 (2)	3 (2)	6 (1)	−1 (1)	−18 (1)	63 (1)	−81 (3)	42 (1)	105	42 (1)
C(371)	4154 (1)	2923 (1)	−471 (1)	0·55	23 (4)	9 (3)	11 (4)	5 (3)	9 (3)	0 (3)	10 (1)	12 (1)	30 (1)	78 (1)	68 (1)	72 (1)	86	7 (1)
C(372)	4682 (1)	3504 (1)	−890 (1)	0·45	32 (5)	37 (5)	31 (6)	24 (4)	−2 (5)	−6 (5)	−3 (1)	−4 (1)	−22 (1)	43 (2)	−47 (2)	55 (1)	105	55 (1)
C(381)	4220 (1)	2986 (1)	−2707 (1)	0·55	9 (3)	20 (3)	20 (4)	9 (3)	5 (3)	8 (3)	9 (1)	14 (1)	31 (1)	−11 (1)	−20 (1)	81 (1)	86	17 (1)
C(382)	3912 (1)	2773 (1)	−2565 (1)	0·45	17 (4)	10 (4)	30 (5)	2 (3)	0 (4)	−1 (4)	8 (1)	14 (1)	8 (1)	5 (1)	11 (1)	37 (3)	105	67 (1)
C(391)	3660 (1)	3498 (1)	−5957 (1)	0·55	27 (4)	32 (4)	15 (4)	7 (3)	10 (3)	12 (3)	−1 (1)	11 (1)	24 (1)	72 (8)	11 (2)	3 (1)	86	25 (1)
C(392)	3667 (1)	3782 (1)	−5215 (1)	0·45	28 (5)	43 (5)	19 (5)	6 (4)	3 (4)	21 (4)	4 (1)	14 (1)	32 (1)	−18 (3)	74 (1)	70 (1)	105	71 (1)
C(401)	2632 (1)	2555 (1)	−4526 (1)	0·55	6 (3)	11 (4)	31 (5)	0 (3)	10 (3)	12 (3)	7 (1)	14 (1)	37 (2)	1 (1)	82 (1)	8 (1)	86	25 (1)
C(402)	2402 (1)	2579 (1)	−4619 (1)	0·45	19 (5)	42 (7)	26 (5)	−2 (5)	7 (4)	0 (5)	7 (1)	16 (1)	8 (2)	−20 (1)	23 (1)	75 (5)	105	74 (1)
N(1)	−733 (1)	−4383 (1)	−6379 (1)	1·00	25 (2)	20 (2)	28 (2)	2 (1)	7 (2)	2 (1)	4 (1)	1 (1)	2 (2)	91 (4)	72 (29)	0 (14)		
C(2)	−275 (1)	−3500 (1)	−5719 (1)	1·00	20 (2)	19 (2)	20 (2)	8 (1)	8 (2)	5 (2)	4 (1)	1 (2)	2 (3)	81 (5)	−20 (21)	74 (18)		
C(3)	257 (1)	−2375 (1)	−4916 (1)	1·00	19 (2)	13 (2)	13 (2)	3 (1)	3 (2)	3 (1)	4 (1)	1 (1)	3 (2)	74 (4)	71 (21)	73 (13)		
C(4)	−220 (1)	−1566 (1)	−4595 (1)	1·00	15 (2)	13 (2)	16 (2)	0 (1)	3 (2)	3 (1)	5 (1)	2 (1)	4 (2)	69 (4)	52 (12)	75 (10)		
N(5)	−643 (1)	−969 (1)	−4364 (1)	1·00	21 (2)	18 (2)	29 (2)	4 (1)	6 (2)	4 (1)	5 (1)	0 (1)	4 (2)	67 (3)	21 (86)	80 (9)		
C(6)	1131 (1)	−2105 (1)	−4515 (1)	1·00	17 (2)	14 (2)	13 (2)	5 (1)	4 (2)	4 (1)	5 (1)	0 (1)	4 (2)	71 (4)	14 (22)	65 (10)		
C(7)	1649 (1)	−965 (1)	−3730 (1)	1·00	21 (2)	10 (2)	14 (2)	5 (1)	4 (2)	2 (1)	5 (1)	2 (1)	3 (2)	63 (4)	60 (12)	60 (13)		
C(8)	2509 (1)	−712 (1)	−3329 (1)	1·00	20 (2)	12 (2)	16 (2)	3 (1)	3 (2)	3 (1)	4 (1)	3 (1)	1 (3)	62 (4)	78 (8)	94 (28)		
C(9)	2942 (1)	−1574 (1)	−3701 (1)	1·00	16 (2)	17 (2)	14 (2)	6 (1)	3 (2)	5 (1)	5 (1)	3 (1)	−3 (2)	67 (4)	85 (8)	66 (11)		
C(10)	2428 (1)	−2709 (1)	−4472 (1)	1·00	19 (2)	13 (2)	14 (2)	6 (1)	4 (2)	2 (1)	5 (1)	2 (1)	−4 (2)	80 (3)	92 (11)	77 (9)		
C(11)	1570 (1)	−2965 (1)	−4850 (1)	1·00	19 (2)	11 (2)	17 (2)	4 (1)	5 (2)	4 (1)	5 (1)	−1 (1)	1 (3)	83 (3)	31 (12)	−9 (54)		
N(12)	4537 (1)	−2931 (1)	−4011 (1)	1·00	24 (2)	33 (2)	42 (3)	14 (2)	4 (2)	10 (2)	5 (1)	6 (1)	−23 (2)	77 (3)	85 (3)	71 (2)		
C(13)	4239 (1)	−2207 (1)	−3697 (1)	1·00	14 (2)	25 (2)	26 (2)	3 (2)	2 (2)	7 (2)	4 (1)	6 (1)	−15 (2)	74 (4)	86 (4)	67 (3)		
C(14)	3826 (1)	−1328 (1)	−3344 (1)	1·00	20 (2)	15 (2)	19 (2)	5 (2)	2 (2)	5 (2)	4 (1)	5 (1)	−9 (2)	65 (4)	82 (5)	64 (4)		
C(15)	4367 (1)	−203 (1)	−2604 (1)	1·00	15 (2)	26 (2)	30 (2)	10 (1)	4 (2)	9 (2)	5 (1)	6 (1)	−9 (2)	55 (4)	71 (4)	52 (4)		
N(16)	4791 (1)	693 (1)	−2024 (1)	1·00	23 (2)	23 (2)	53 (3)	4 (2)	2 (2)	6 (2)	4 (1)	5 (1)	−12 (2)	49 (3)	67 (4)	48 (3)		
N(17)	−1938 (1)	−4843 (1)	−2346 (1)	1·00	25 (2)	19 (2)	51 (2)	3 (2)	16 (2)	−3 (2)	6 (1)	2 (1)	−9 (2)	72 (3)	67 (11)	46 (4)		
C(18)	−1503 (1)	−3955 (1)	−1541 (1)	1·00	16 (2)	19 (2)	25 (2)	7 (1)	10 (2)	5 (2)	6 (1)	3 (1)	11 (2)	67 (3)	64 (9)	87 (3)		
C(19)	−1006 (1)	−2832 (1)	−595 (1)	1·00	18 (2)	9 (2)	18 (2)	4 (1)	5 (2)	1 (1)	6 (1)	0 (1)	6 (3)	61 (3)	15 (29)	77 (7)		
C(20)	−1486 (1)	−2055 (1)	−138 (1)	1·00	19 (2)	14 (2)	16 (2)	−1 (2)	3 (2)	3 (2)	6 (1)	1 (1)	−4 (3)	55 (3)	41 (29)	26 (8)		
N(21)	−1903 (1)	−1454 (1)	232 (1)	1·00	24 (2)	15 (2)	29 (2)	6 (1)	8 (1)	5 (1)	5 (1)	0 (1)	5 (2)	50 (3)	20 (14)	69 (7)		
C(22)	−107 (1)	−2523 (1)	−160 (1)	1·00	19 (2)	15 (2)	11 (2)	3 (2)	4 (2)	4 (1)	5 (1)	−1 (1)	2 (3)	55 (4)	84 (10)	−22 (26)		
C(23)	365 (1)	−1386 (1)	655 (1)	1·00	19 (2)	13 (2)	16 (2)	7 (1)	5 (2)	4 (1)	5 (1)	2 (2)	0 (2)	49 (3)	26 (12)	−12 (43)		
C(24)	1237 (1)	−1081 (1)	1078 (1)	1·00	22 (2)	11 (2)	13 (2)	4 (1)	3 (2)	2 (1)	5 (1)	4 (1)	−3 (3)	46 (3)	27 (6)	80 (9)		
C(25)	1708 (1)	−1882 (1)	751 (1)	1·00	18 (2)	15 (2)	12 (2)	4 (1)	3 (2)	4 (1)	5 (1)	3 (1)	5 (2)	51 (3)	37 (7)	29 (8)		
C(26)	1233 (1)	−3024 (1)	−48 (1)	1·00	22 (2)	15 (2)	15 (2)	7 (1)	5 (2)	5 (1)	5 (1)	3 (1)	2 (3)	55 (3)	37 (7)	31 (17)		
C(27)	359 (1)	−3328 (1)	−493 (1)	1·00	21 (2)	10 (2)	15 (2)	3 (1)	4 (2)	2 (1)	6 (1)	2 (1)	0 (2)	58 (3)	44 (12)	66 (32)		
N(28)	3449 (1)	−3020 (1)	478 (1)	1·00	28 (2)	23 (2)	41 (2)	10 (2)	10 (2)	12 (2)	9 (1)	10 (1)	9 (2)	52 (2)	41 (2)	42 (4)		
C(29)	3083 (1)	−2361 (1)	813 (1)	1·00	19 (2)	17 (2)	22 (2)	0 (2)	3 (2)	7 (2)	6 (1)	7 (1)	6 (2)	49 (3)	33 (3)	38 (6)		
C(30)	2607 (1)	−1565 (1)	1179 (1)	1·00	16 (2)	18 (2)	15 (2)	5 (1)	3 (2)	6 (1)	6 (1)	4 (1)	6 (2)	49 (3)	30 (5)	27 (7)		
C(31)	3089 (1)	−422 (1)	2012 (1)	1·00	18 (2)	24 (2)	21 (2)	7 (2)	7 (2)	5 (2)	5 (1)	−4 (1)	9 (3)	40 (3)	67 (4)	23 (4)		
N(32)	3462 (1)	497 (1)	2699 (1)	1·00	22 (2)	22 (2)	35 (2)	4 (1)	6 (2)	3 (2)	5 (1)	−6 (1)	10 (2)	39 (3)	63 (3)	20 (4)		

	x	y	z	p	U_{iso} ($Å^2 \times 10^2$)
H(341)	4078	5069	−2181	0·55	2 (2)
H(342)	2952	4680	−2922	0·55	0 (2)
H(343)	2790	3735	−838	0·45	10 (5)
H(344)	2858	4706	−2359	0·45	12 (5)
H(351)	2906	3727	−85	0·55	2 (2)
H(352)	3497	5135	970	0·55	3 (2)
H(353)	4362	5407	−757	0·45	7 (4)
H(354)	3793	5379	1297	0·45	8 (4)
H(371)	4696	2669	182	0·55	2 (2)
H(372)	3570	2330	−478	0·55	2 (2)
H(373)	5039	2996	−261	0·45	3 (3)
H(374)	5071	4011	−1677	0·45	332 (203)
H(381)	4152	2158	−3682	0·55	11 (4)
H(382)	4832	3525	−2691	0·55	0 (2)
H(383)	4075	2236	−3864	0·45	0 (2)
H(384)	3563	2274	−1696	0·45	5 (3)
H(391)	4284	4081	−5629	0·55	3 (2)
H(392)	3181	3846	−6637	0·55	2 (2)
H(393)	3650	2732	−7072	0·55	9 (4)
H(394)	3243	4196	−5920	0·45	2 (2)
H(395)	4261	4386	−4341	0·45	5 (3)
H(396)	3792	3168	−6458	0·45	11 (5)
H(401)	2465	2360	−3108	0·55	2 (2)
H(402)	2636	1803	−5660	0·55	13 (5)
H(403)	2167	2918	−5226	0·55	7 (3)
H(404)	1966	2976	−5326	0·45	4 (3)
H(405)	2507	1939	−5850	0·45	2 (3)
H(406)	2133	2210	−3468	0·45	15 (6)
H(7)	1342	−302	−3456	1·00	2 (1)
H(8)	2880	147	−2722	1·00	3 (1)
H(10)	2737	−3369	−4752	1·00	2 (1)
H(11)	1202	−3828	−5412	1·00	4 (1)
H(23)	29	−754	942	1·00	2 (1)
H(24)	1577	−209	1678	1·00	3 (1)
H(26)	1568	−3658	−303	1·00	2 (1)
H(27)	15	−4198	−1112	1·00	3 (1)

the channels by the shifting of the TCNQ molecules parallel to **a** by about ±0·1 Å. Another feature is the twisting around **c** of TCNQ *A* and TCNQ *B* in opposite senses, which is caused by rather large displacements parallel to **b** (up to ±0·1 Å) in the regions where the TCNQ stacks are in contact *via* the cyano groups. The component of the modulation wave parallel to **c** (about 0·1 Å) modulates the bending out of the molecular plane of the cyano groups, a bending which can be found for most of the other TCNQ complexes too [up to 0·45 Å, for example, for DMM(TCNQ)$_2$(I) at 95 K; Middeldorp *et al.* (1985)].

There are several possible mechanisms by which a structure can become (in)commensurately modulated. For the quasi-one-dimensional organic compounds of which DMM(TCNQ)$_2$(II) is an example, the first mechanism which comes to mind is that of a Peierls distortion (Peierls, 1955) of the TCNQ chains. However, the DMM ions have a single positive charge and consequently the TCNQ band is quarterly filled. Therefore, if charge density wave (CDW) formation is the driving mechanism of the distortion, one would expect a doubling of the unit cell along the stack axis. This is not what is found experimentally, and the CDW mechanism cannot be used to explain the incommensurateness of the modulation.

Although not the driving force, the modulation on the TCNQ chain (rotation and translation of neighbouring molecules with respect to each other) does give rise to a variation of the transfer integrals (van Smaalen & Kommandeur, 1985; van Smaalen, Kommandeur & Conwell, 1986) and presumably to the occurrence of a gap in the valence band. However, this gap will not be at the Fermi level and a dramatic effect on the electrical conductivity, *i.e.* a metal–insu-

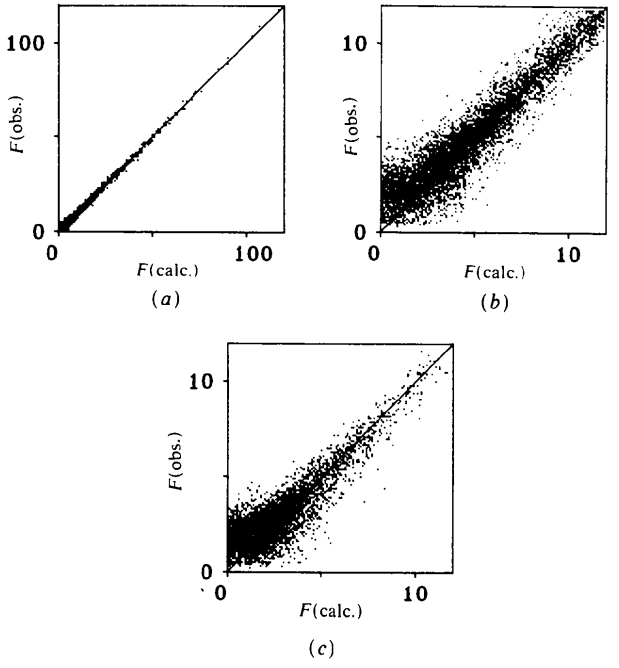

Fig. 4. F(obs.)/F(calc.) plots for (*a*) the main reflections, (*b*) the main reflections on the same scale as (*c*) the first-order satellite reflections. The distributions in (*b*) and (*c*) are quite similar.

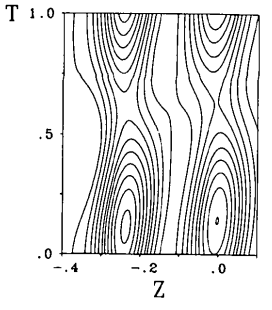

Fig. 5. Section through the (3+1)-FF for the atom pair C(341)–C(351) (belonging to DMM-1). The simultaneous occurrence of both a density and a shift modulation is shown.

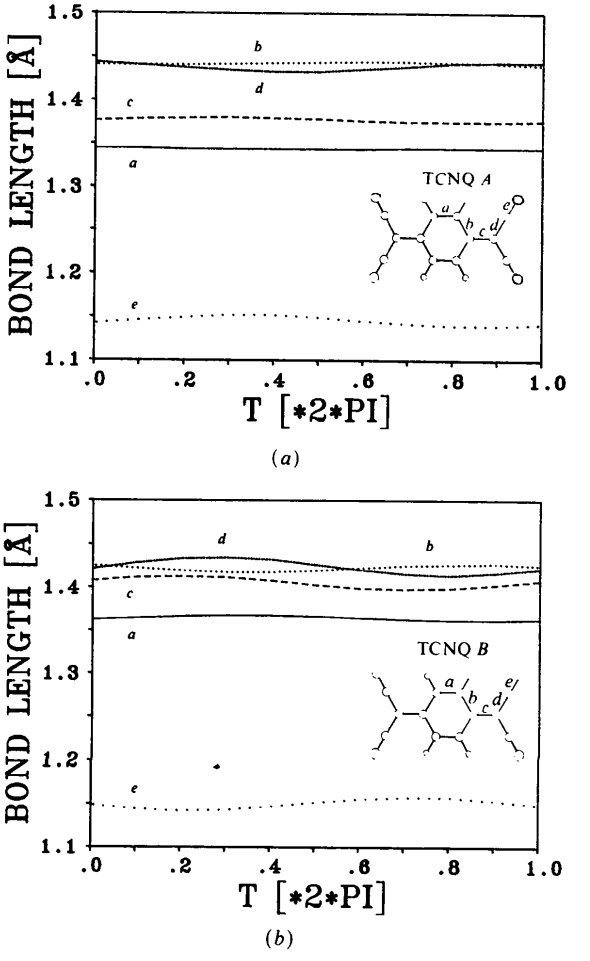

Fig. 6. Some characteristic bond lengths in the molecules (*a*) TCNQ *A* (including atoms with numbers 1–16) and (*b*) TCNQ *B* (atoms with numbers 17–32) during one modulation period. The plotted distances correspond to those marked on the insert, the e.s.d.'s are about ±0·03–0·04 Å.

lator transition, is not to be expected. This is in full accordance with the experimental findings (Oostra, 1985).

A second explanation for the incommensurateness of the modulation would be to assume the existence of + and − domains, corresponding to the DMM-1 and DMM-2 conformations, of fluctuating size, giving on average an incommensurate **q** vector. Higher-order satellites would disappear because of the rather high degree of randomness (Fujiwara, 1957). However, for a reasonable microdomain model of the type mentioned above, one would expect a simple **q** direction, *e.g.* perpendicular to the TCNQ stacks, and not a general direction as is actually observed.

Further models to explain the modulation include the assumption of special forms of the intermolecular interaction, that is forces beyond the harmonic approximation and/or the inclusion of second- and higher-order nearest-neighbour interactions (Janssen, 1986). Also, a soliton lattice can be considered (Perez-Mato & Madariaga, 1986). However, the most likely origin lies in the steric hindrance between the TCNQ stacks and the DMM molecules. This can be understood when one realizes the analogy with intergrowth structures (Janner & Janssen, 1980). An example of the latter is mercury arsenic hexafluoride (Pouget, Shirane, Hasting, Heeger, Miro & MacDiarmid, 1978). The incommensurability occurs owing to the presence of two interpenetrating lattices. For $Hg_{3-x}AsF_6$, there is a host lattice given by the AsF_6 units. The Hg atoms are dispersed homogeneously in channels in this host lattice. The result is that at high temperatures the Hg atoms are disorderly dispersed in the channels, whereas at low temperatures they form an incommensurate structure.

Completely analogously, in $DMM(TCNQ)_2$(II) we can identify a lattice defined by the TCNQ molecules and channels filled by DMM groups. At high temperatures, the spacing between the TCNQ molecules is large enough to accommodate dynamically disordered DMM groups. Owing to the relatively large shrinkage on cooling (van Smaalen, de Boer, Haas & Kommandeur, 1985), DMM has less space available at lower temperatures. Apparently, the DMM groups do not fit into the TCNQ lattice, and a modulated structure is the result.

From an energetic point of view, an intergrowth structure becomes incommensurate in order to minimize the elastic energy. By means of the (incommensurate) modulation, large destabilizing terms in the lattice energy (Born repulsion) are avoided, while the molecules remain close enough for van der Waals

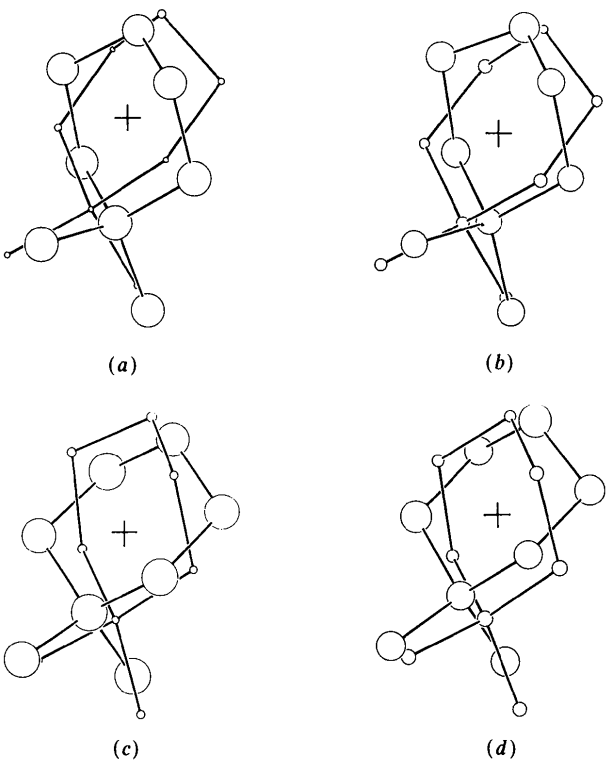

Fig. 7. *ORTEP* plots (Johnson, 1965) of both possible DMM chair conformations (projected along **a**). The size of the circles is proportional to the actual occupancy of the respective atom position, a reference point is marked by a cross. The phase terms of the modulation are (*a*) $T=0$, (*b*) $T=0{\cdot}25$, (*c*) $T=0{\cdot}5$ and (*d*) $T=0{\cdot}75$.

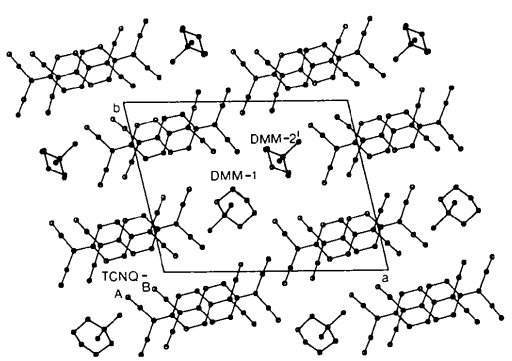

Fig. 8. Projection of the crystal structure of $DMM(TCNQ)_2$(II) at 99 K parallel to **c**. The loss of translation symmetry is evident, see, for example, successive DMM groups along **b**.

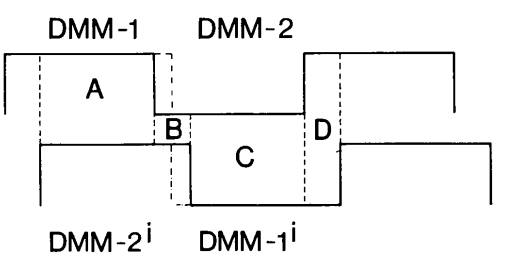

Fig. 9. Schematic drawing of both centrosymmetrically equivalent DMM modulation functions. The regions *A*, *C* and *D* represent sterically possible combinations of neighbouring DMM molecules. The energetically unfavourable case *B* can be avoided if, for example, an asymmetric wave (dash-dotted line) is chosen. Then *B* is replaced by extended areas of *A* and *C*.

binding. To obtain this minimum in the energy in a model calculation, it would now be sufficient to consider only nearest-neighbour interactions.

As to physical properties, the incommensurate modulation appears not to have a strong effect on the electrical conductivity. As mentioned above, no anomaly has been observed around 200 K (Oostra, 1985), the temperature where the modulation sets in. The effects of the modulation are, however, noticeable in the magnetic susceptibility. Above about 10 K the compound behaves as a normal one-dimensional $S = \frac{1}{2}$ antiferromagnet with a spin-spin exchange constant of 7 K (Korving, Hijmans, Brom, Oostra, Sawatzky & Kommandeur, 1983). The expected maximum at 9 K in the magnetic susceptibility (Bonner & Fisher, 1964) is, however, entirely absent and the magnetic susceptibility rises steadily down to 1·65 K, where a phase transition occurs. The overall shape of the magnetic susceptibility curve resembles that of a spin glass. As noted by Hijmans (1985), this probably indicates a distribution of exchange constants along the TCNQ chains. This phenomenon can be understood when one takes into account the influence of the incommensurate periodic potential of the DMM ions on the TCNQ chains. The exchange constants along the TCNQ chains will follow this modulation and this is not a minor effect since exchange constants are quite sensitive to the magnitude of a periodic potential (Kramer & Brom, 1984).

The authors thank Dr S. Oostra for valuable discussions. One of us (RJJV) acknowledges the Netherlands Foundation for Chemical Research (SON).

References

ADLHART, W. (1982). *Acta Cryst.* A**38**, 498-504.
BOER, J. L. DE & DUISENBERG, A. J. M. (1984). Enraf-Nonius CAD-4F diffractometer software, updated February 84. Groningen, Utrecht, The Netherlands.
BONNER, J. C. & FISHER, M. E. (1964). *Phys. Rev. A*, **135**, 640-658.
FUJIWARA, K. (1957). *J. Phys. Soc. Jpn*, **12**, 7-17.
HELMHOLDT, R. B. & VOS, A. (1977). *Acta Cryst.* A**33**, 456-465.
HIJMANS, T. W. (1985). Thesis, Univ. of Leiden.
International Tables for X-ray Crystallography (1974). Vol. IV. Birmingham: Kynoch Press. (Present distributor D. Reidel, Dordrecht.)
JANNER, A. & JANSSEN, T. (1980). *Acta Cryst.* A**36**, 408-415.
JANSSEN, T. (1986). *Microscopic Theories of Incommensurate Crystal Phases.* In *Incommensurate Phases in Dielectrics*, Part I, *Fundamentals*, edited by R. BLINC & A. P. LEVANYUK. Amsterdam: North-Holland.
JOHNSON, C. K. (1965). *ORTEP.* Report ORNL-3794. Oak Ridge National Laboratory, Tennessee, USA.
KAMMINGA, P. & VAN BODEGOM, L. (1981). *Acta Cryst.* B**37**, 114-119.
KORVING, W. H., HIJMANS, T. W., BROM, H. B., OOSTRA, S., SAWATZKY, G. A. & KOMMANDEUR, J. (1983). *J. Phys. (Paris)*, C**44**, 1425.
KRAMER, G. J. & BROM, H. B. (1984). *Mol. Cryst. Liq. Cryst.* **120**, 153.
MELBY, L. R., HARDER, A. J., HERTLER, W. R., MAHLER, W., BENSON, R. & MOCHEL, W. E. (1982). *J. Am. Chem. Soc.* **84**, 3370.
MIDDELDORP, J. A. M., VISSER, R. J. J. & DE BOER, J. L. (1985). *Acta Cryst.* B**41**, 369-374.
OOSTRA, S. (1985). Thesis, Univ. of Groningen, The Netherlands.
PEIERLS, R. E. (1955). *Quantum Theory of Solids.* Oxford Univ. Press.
PEREZ-MATO, J. M. & MADARIAGA, G. (1986). *Solid State Commun.* **58**, 105-109.
POUGET, J. P., SHIRANE, G., HASTING, J. M., HEEGER, A. J., MIRO, N. D. & MACDIARMID, A. G. (1978). *Phys. Rev. B*, **18**, 3645-3656.
SHELDRICK, G. M. (1976). *SHELX*76. Program for crystal structure determination. Univ. of Cambridge, England.
SMAALEN, S. VAN, DE BOER, J. L., HAAS, C. & KOMMANDEUR, J. (1985). *Phys. Rev. B*, **31**, 3496-3503.
SMAALEN, S. VAN & KOMMANDEUR, J. (1985). *Phys. Rev. B*, **31**, 8056-8060.
SMAALEN, S. VAN, KOMMANDEUR, J. & CONWELL, E. M. (1986). *Phys. Rev. B*, **33**, 5378-5383.
STEURER, W. (1987). *Acta Cryst.* A**43**, 36-42.
STEURER, W. & ADLHART, W. (1983). *Acta Cryst.* B**39**, 349-355.
VISSER, R. J. J., DE BOER, J. L. & VOS, A. (1987). In preparation.
VISSER, R. J. J., VAN HEEMSTRA, T. W. L. & DE BOER, J. L. (1982). *Mol. Cryst. Liq. Cryst.* **85**, 265-269.
WOLFF, P. M. DE (1974). *Acta Cryst.* A**30**, 777-785.

Acta Cryst. (1987). B**43**, 574-579

Application of the HOSE (Harmonic Oscillator Stabilization Energy) Model to Y-Shaped Molecules

BY JANINA KAROLAK-WOJCIECHOWSKA

Institute of General Chemistry, Technical University, Żwirki 36, 90-362 *Łódź, Poland*

(*Received* 6 *November* 1986; *accepted* 7 *July* 1987)

Abstract

The HOSE model has been applied to molecules containing the Y-shaped π-electron fragment of the thiourea (or urea) molecule. The contributions of the resonance structures (c_i) for this fragment of the molecules and the value of the stabilization energy (E_{HOSE}) have been estimated from bond lengths determined by X-ray methods. On the basis of these values relationships between the structures and

0108-7681/87/060574-06$01.50